Biosensors and Bioelectronics 68 (2015) 382–389

Contents lists available at ScienceDirect

Biosensors and Bioelectronics

journal homepage: www.elsevier.com/locate/bios

Label-free impedance detection of cancer cells from whole blood on an integrated centrifugal microfluidic platform

Charles E. Nwankire [a,b,*,1], Anita Venkatanarayanan [a,c,1], Thomas Glennon [a,b], Tia E. Keyes [a,c], Robert J. Forster [a,c], Jens Ducrée [a,b,*]

[a] Biomedical Diagnostics Institute, National Center for Sensor Research, Dublin City University, Ireland
[b] School of Physical Sciences, Dublin City University, Ireland
[c] School of Chemical Sciences, Dublin City University, Ireland

ARTICLE INFO

Article history:
Received 13 October 2014
Received in revised form
15 December 2014
Accepted 22 December 2014
Available online 30 December 2014

Keywords:
Electrochemical
Label-free detection
Impedance
Centrifugal microfluidics
Lab-on-a-Disc
Circulating tumour cells
Cancer
EpCAM
Biosensor
Immunoassay

ABSTRACT

An electrochemical Lab-on-a-Disc (eLoaD) platform for the automated quantification of ovarian cancer cells (SKOV3) from whole blood is reported. This centrifugal microfluidic system combines complex sample handling, i.e., blood separation and cancer cell extraction from plasma, with specific capture and sensitive detection using label-free electrochemical impedance. Flow control is facilitated using rotationally actuated valving strategies including siphoning, capillary and centrifugo-pneumatic dissolvable-film (DF) valves. For the detection systems, the thiol-containing amino acid, L-Cysteine, was self-assembled onto smooth gold electrodes and functionalized with anti-EpCAM. By adjusting the concentration of buffer electrolyte, the thickness of the electrical double layer was extended so the interfacial electric field interacts with the bound cells. Significant impedance changes were recorded at 117.2 Hz and 46.5 Hz upon cell capture. Applying AC amplitude of 50 mV at 117.2 Hz and open circuit potential, a minimum of 214 captured cells/mm^2 and 87% capture efficiency could be recorded. The eLoaD platform can perform five different assays in parallel with linear dynamic range between 16,400 and $(2.6 \pm 0.0003) \times 10^6$ cancer cells/mL of blood, i.e. covering nearly three orders of magnitude. Using the electrode area of 15.3 mm^2 and an SKOV3 cell radius of 5 μm, the lower detection limit is equivalent to a fractional surface coverage of approximately 2%, thus making eLoaD a highly sensitive and efficient prognostic tool that can be developed for clinical settings where ease of handling and minimal sample preparation are paramount.

1. Introduction

Metastasis is the main cause of cancer-related deaths worldwide and it is estimated to rise over 20 million in 2030 according to World Health Organization (Jemal et al., 2011). Progression of the disease is the result of a multistage process during which circulating tumour cells (CTCs) typically detach from the primary tumour site and circulate in the blood stream. These CTCs tend to be very rare (Sheng et al., 2012); it is often assumed their concentration may be as low as ~1–100 cells/mL in whole blood (Coumans et al., 2013; Hou et al., 2013). Nevertheless, their concentration in blood has (Pantel et al., 2008) diagnostic and prognostic clinical relevance (Dotan et al., 2009; Lianidou et al., 2012; Scher et al., 2009; Wicha and Hayes, 2011). Current methods for the detection and staging of cancer are mostly pathological and provide clinicians with a snapshot of the primary tumour and the spread of cancer from one organ to another, but not necessarily the total tumour burden. This deficit makes it challenging to accurately predict patient outcome or directly guide treatment. Also, chiefly owing to their extremely low concentration, the isolation and detection of CTCs within the human bloodstream make their reliable isolation and detection a highly complex and time consuming task involving expensive instrumentation, resources and highly trained laboratory staff. Capture of (viable) CTCs using inexpensive rapid diagnostics may offer a new way to detect metastasis and prognose patients as well as providing molecular level insights into the genetic profile of the cancer that will guide the selection of the optimum treatment.

CTCs are inherently variable with respect to their density, size, size distribution, morphology, deformability and cell surface composition (Jin et al., 2014), thus demanding a highly flexible capture and detection system. Consequently, techniques including density-gradient based centrifugation (Park et al., 2012), micro-

* Corresponding authors.
E-mail addresses: charles.nwankire@dcu.ie (C.E. Nwankire), jens.ducree@dcu.ie (J. Ducrée).
[1] These authors contributed equally to this work.

http://dx.doi.org/10.1016/j.bios.2014.12.049
0956-5663/

filtration (Zheng et al., 2011), hydrodynamic sorting by size (Loutherback et al., 2012), separation by cell deformability (Tan et al., 2009), immunoassay based on tumour-specific surface protein expression (Alix-Panabieres and Pantel, 2014), and molecular markers (Nagrath et al., 2007) have been employed to effectively separate these cells from normal blood cells before capture. Subsequent enumeration of captured CTCs has been demonstrated with such techniques as immunofluorescence (Ignatiadis et al., 2008), confocal microscopy (Greiner et al., 2011), absorbance (Vila-Planas et al., 2011), chemiluminescence (Hun et al., 2010), interference spectroscopy (Kumeria et al., 2012), surface-enhanced Raman scattering (Lee et al., 2014b) and surface plasmon resonance (Law et al., 2011). However, a simple, sensitive and robust assay that allows routine detection and subsequent molecular characterization of CTCs in a clinical setting has not been reported.

Centrifugal platforms for bioanalytical assays have been investigated for more than 40 years (Ducrée et al., 2007; Gorkin et al., 2010; Madou et al., 2006). For cell separation, these Lab-on-a-Disc (LoaD) platforms excel with respect to more common pressure-driven systems due to the simplified operation without pneumatic interfaces and pumps, the capability for powerful sample preparation and the demonstrated amenability for full integration, automation and parallelization of comprehensive bioanalytical assay protocols (Duford et al., 2013; Focke et al., 2010; Gorkin et al., 2012; Kim et al., 2014; C. Nwankire et al., 2013; Nwankire et al., 2014; C.E. Nwankire et al., 2013). LoaD platforms have also been developed for cell handling, bioassays (Boettcher et al., 2006; Burger and Ducrée, 2012; Burger et al., 2012; Chen et al., 2012; Lee et al., 2014a) and have also been interfaced with electrical systems for real-time flow monitoring (Abi-Samra et al., 2013). For cell detection, electrochemical schemes are beneficial due to their ability to provide highly sensitive, rapid real-time quantitative information, based on simple instrumentation. When combined with electrochemical impedance, electrochemical detection can also be label-free and non-destructive (Venkatanarayanan et al., 2013).

Hence, combining the benefits of electrochemical impedance spectroscopy (EIS) and LoaD platforms, we here demonstrate for the first time, label-free electrochemical detection of ovarian cancer cells in a fully integrated, multiplexed, automated eLoaD platform.

2. Experimental section

2.1. Chemicals and solutions

Sulphuric acid, sulpho-N-hydroxy succinimide (NHS), 1-ethyl-3-[3-dimethyl-amino-propyl] carbodiimide hydrochloride (EDC), 2.5% casein, paraformaldehyde and fetal bovine serum (FBS), L-Cysteine hydrochloride, ethylene diamine tetraacetic acid (EDTA), Ficoll PM 400 were purchased from Sigma-Aldrich and used as received. The SKOV3 ovarian cancer cell line was purchased from ATCC and stored in liquid nitrogen. Details of the cell culture protocol are given in S1-ESI. Purified anti-EpCAM (CD326) antibodies were obtained from Biolegend. McCoy's 5A (containing L-glutamine), penicillin streptomycin (pen/strep), Dulbecco's phosphate buffered saline (DPBS) without calcium and magnesium, as well as trypan blue were all purchased from Fisher Scientific. Accutase cell dissociation buffer was bought from Invitrogen. Experiments involving cells were carried out in a certified Biosafety Level II laboratory under sterile, laminar air flow conditions. Cells were fixed following impedance measurements with 3.5% (w/v) paraformaldehyde. All aqueous solutions were prepared using milli-Q water (18 MΩ cm^{-1}).

2.2. eLoaD fabrication

The eLoaD platform is made up of five layers in total – two adhesive layers were sandwiched between three PMMA polymer layers (Fig. 1A). Computer-Aided-Design (CAD) files of the vents, vias and reservoirs were machined in the 1.5-mm thick PMMA (Radionics, Ireland) layers using a CO_2 laser cutter (Zing 16, Epilog USA). Microchannels were patterned onto the ~90-μm thick pressure sensitive adhesive (Adhesives Research, Ireland) layers using a knife cutter (Graphtec Corp., USA). Sacrificial valves fabricated from water dissolvable films (DFs) and cut with the knife cutter were integrated onto the single-use disc for centrifugal flow control (Gorkin et al., 2012; Nwankire et al., 2014). Five pairs of gold (working and [reference+counter]) electrodes were sputter-coated onto the bottom layer of the disc assembly (Fig. 1). The electrodes were subsequently cleaned individually by electrochemically cycling them in aqueous 0.5 M H_2SO_4 at 100 mV s^{-1} from +0.2 V to 1.6 V vs. Ag/AgCl (3 M saturated KCl) reference

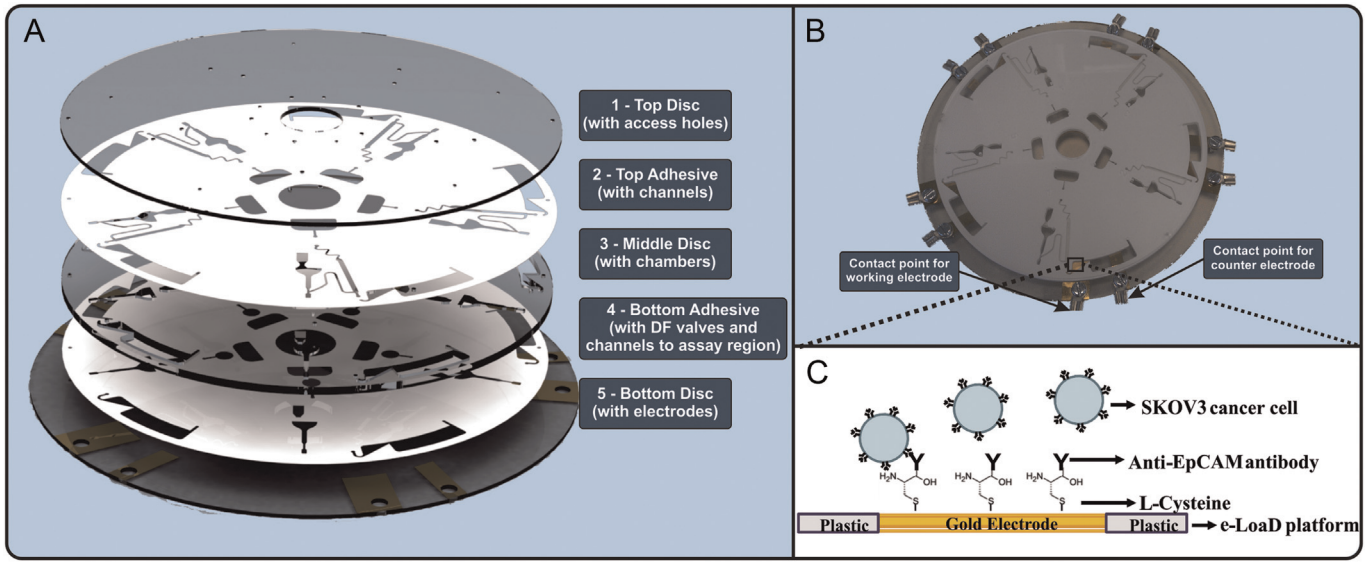

Fig. 1. (A) Rendered 3D image of the 5-layer microfluidic disc platform comprising of three 1.5-mm thick PMMA discs and two ~90-μm thick pressure sensitive adhesive films. The gold electrodes were deposited on the bottom (layer 5) disc. (B) Fully assembled disc showing contact points for the working and counter electrodes. (C) Schematic of electrochemical rare cell capture assay on polymeric eLoaD platform.

electrode until a stable gold reduction peak was obtained.

2.3. Immobilization of capture antibody on gold electrodes

Following acid cleaning, the gold electrodes were thoroughly washed with deionized water and 50 μL drop of 1 mM aqueous L-Cysteine hydrochloride solution was placed on the working electrodes. The monolayer was allowed to self-assemble for 7 h in the dark. After the formation of the monolayer, the discs were rinsed thoroughly with 0.01-M DPBS and dried under a nitrogen stream. Following monolayer assembly the working electrodes were activated with 50 μL drop of 5 mM sulpho NHS-EDC for 15 min. This was followed by incubation of the activated gold electrodes with a 50 μL droplet of 100 μg/mL anti-EpCAM antibody solution for 3 h at room temperature. Fig. 1C shows the schematic diagram of the capture surface. The antibody-coated electrodes were washed thoroughly with DPBS and the entire bottom disc (layer 5, Fig. 1A) was incubated in 2.5% casein solution for 30 min to block any bare electrode and exposed disc surface. After 30 min, this layer was thoroughly rinsed with DPBS and dried under nitrogen stream. Finally, the five layers and the DF valves were subsequently aligned and assembled (Fig. 1B) using a custom-made alignment jig and a hydraulic laminator. Anti-EpCAM (Park et al., 2012) was immobilized on gold electrodes to specifically capture SKOV3 ovarian cancer cells used in this study, due to their high EpCAM expression. In order to target a wider range of cancer cells, we propose immobilizing a panel of specific antibodies on the electrode surface.

2.4. Impedance spectroscopy

Impedance spectroscopy was performed on the two on-disc gold electrodes using a CH Instruments, Model 760D potentiostat inside a Faraday cage. An AC excitation signal of 50 mV (peak-to-peak amplitude) was applied to the electrodes at open circuit potential (OCP) and the frequency of the signal was varied between 0.5 Hz and 100 kHz. All electrochemical measurements were run at room temperature (22 ± 2 °C) using a 2-electrode system with a gold electrode as working and gold electrode as pseudo [reference+counter] electrode unless otherwise stated (Fig. 1B). The dyed cells were imaged using a Zeiss LSM 510 Meta laser module confocal microscope at an excitation wavelength of 488 nm and 10 × magnification objective.

2.5. CTC assay in whole blood on the eLoaD platform

SKOV3 cells were harvested at 70% confluence, 72 h after seeding by brief exposure to 5 mL, 1 × accutase followed by approximately 20-min recovery in DPBS. 3 mL of human blood sample was diluted 50% by addition of 0.1 M EDTA in 0.001 M PBS. The blood samples were obtained from healthy donors, having signed informed consent. Approval for use of blood for these experiments was obtained from the university ethics committee. Cell mixtures were prepared by adding various concentrations of cultured SKOV3 cells to calculated aliquots of fresh 0.1 M EDTA-anticoagulated and diluted human blood to achieve final concentrations between 1.9×10^5 and 1.9×10^8 cells/mL. The SKOV3 cells were pre-stained with 5 μM $DiOC_6$ cell dye. 20 μL of each of the five different cancer cell concentrations were spiked in whole blood and pre-loaded in the five chambers on-disc, along with 15 μL of density gradient medium (Ficoll-Paque, Radionics, Ireland). Next, 65 μL of 0.001 M PBS wash buffer was introduced into their respective chambers. The discs were spun on a centrifugal test stand, which has been described previously elsewhere (Grumann et al., 2005; C. Nwankire et al., 2013). This test stand comprises a computer-controlled motor and a stroboscopic light that is triggered by the disc rotation in order to enable imaging of a particular section of the disc. The cell mixtures were allowed to flow to the reaction chamber and then incubated for 3 h at room temperature by maintaining disc rotation at 1500 rpm. This was followed by a DPBS wash to remove any non-specifically bound cells. Following capture, the change in impedance was recorded in all 5 chambers. Captured cells were then fixed with 100 μL of 3.5% paraformaldehyde for 30 min then washed thoroughly with DPBS, and imaged using confocal microscopy. In order to determine the number of cells captured, cells on a 500 μm × 500 μm area were counted using ImageJ software and normalized to area of the electrode.

3. Results and discussion

3.1. Blood separation and cancer cell extraction

The eLoaD microfluidic platform was designed to enable full integration and automation of laboratory unit operations (LUOs), e.g. blood separation, band extraction of cells, incubation and wash steps, which are required for this immunoassay. Several flow controls and valving techniques including centrifugo-pneumatic DF valves and siphoning were investigated in order to minimize loss of the rare target cells. Density gradient medium has previously been implemented on a LoaD platform for blood stratification (Kinahan et al., 2014). We also observed significant loss of target cells at the blood–plasma interface during fractionation in absence of density gradient medium. Furthermore, loss of target cells was also observed when the blood sample was not slowly layered over the medium (Fig. S2 – ESI). Although the blood separation chamber was re-designed to include a circulating air vent channel positioned directly at the Ficoll–blood interface to re-channel air and facilitate 'smooth layering', some target cells were lost in the pneumatic chamber of the DF valves (Fig. S3 – ESI). To this end, the capillary-based siphon valving strategy was implemented for extraction of the target cancer cells (C.E. Nwankire et al., 2013; Siegrist et al., 2010) (Fig. 2). The spinning protocol that was applied for both the DF and siphon valving strategies are given in Table 1.

In centrifugo-pneumatic DF valves, an air pocket is trapped between a DF membrane on the outer end and a rotationally pressurized liquid plug on the upstream side. Upon reaching a critical burst pressure, the metastable (inverted) air–liquid layer collapses, and liquid makes contact and dissolves the DF, thus clearing the passage for the liquid (Gorkin et al., 2012). Siphon valves, on the other hand, are low-pass valves which yield at low rotational frequencies (C.E. Nwankire et al., 2013; Siegrist et al., 2010).

After completion of blood separation, the supernatant layer containing the white blood cells, platelets and spiked cancer cells primes the siphon channels and continues over the gold working electrode. Cells were incubated by maintaining disc rotation at 1500 rpm for about 3 h. The wash buffer was released by actuating the corresponding DF valve at 3300 rpm. The disc was subsequently stopped to measure electrochemical impedance for each compartment individually and data for a calibration curve collected.

3.2. Electrochemical characterization

The adsorption of biomolecules such as antibodies or cells alters the electrical environment close to the electrode surface (Bard and Faulkner, 2001).

Cyclic voltammetry of an electroactive probe in solution, e.g., ferrocenemethanol (FeMeOH), can provide significant insights into

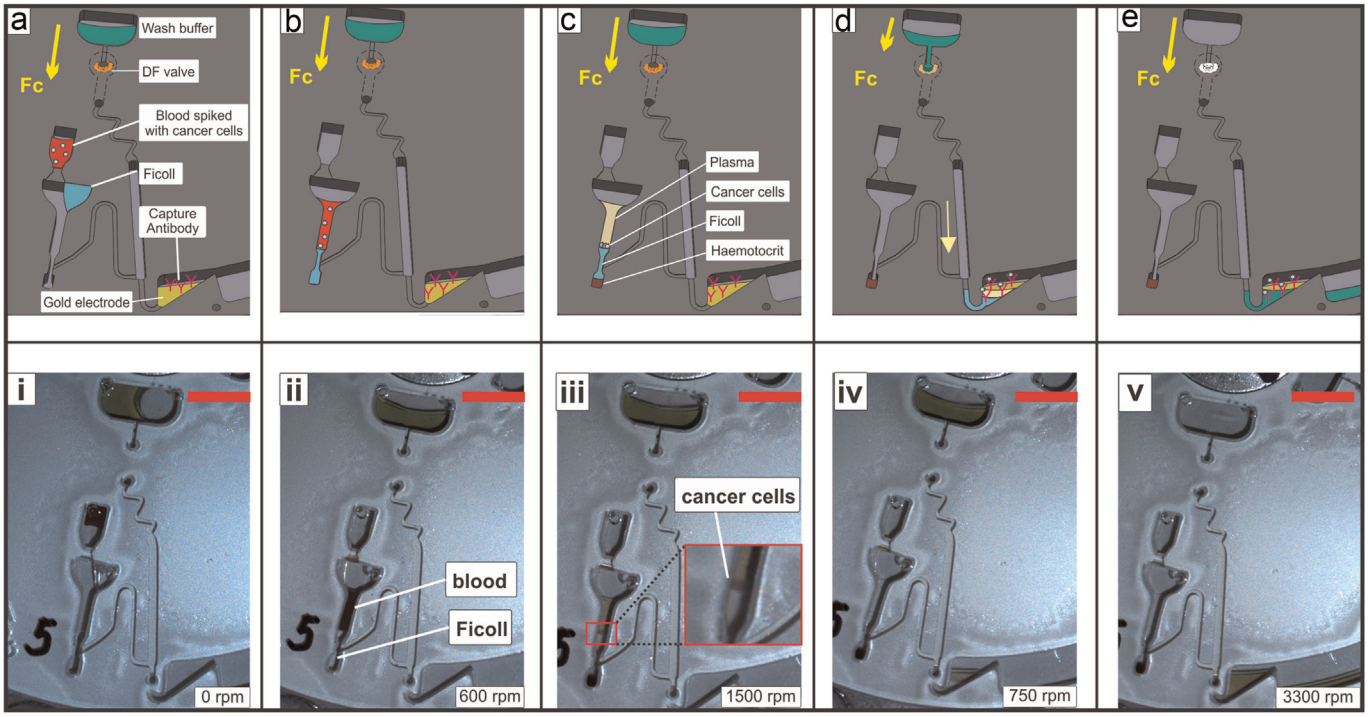

Fig. 2. Schematic (a–e) and image sequence (i–v) of the full assay protocol. (a, i) Highlights the different regions on the disc including the wash buffer, DF valve, whole blood spiked with cancer cells, Ficoll and capture antibody immobilized on the gold electrode. (b, ii) Sample layered over Ficoll at 600 rpm. (c, iii) Blood fractionation completed at 1500 rpm and cancer cells layered at the interface between the Ficoll layer and the plasma. Inset shows the cancer cells at the interface. (d, iv) Siphon priming and extraction of the target cells (inset arrow indicates flow through the siphon channels) and incubation at the electrode region at 750 rpm. (e, v) Wash buffer released and subsequent electrochemical impedance detection; green food dye was used in this image to represent wash buffer to aid visualization. The yellow arrows indicate direction of the centrifugal force (Fc). Red scale bar is 5 mm. (For interpretation of the references to colour in this figure legend, the reader is referred to the web version of this article.)

Table 1
Spin protocol for cancer cell extraction from whole blood.

Laboratory unit operation	Frequency for DF valve actuation [rpm]	Frequency for siphoning [rpm]
Layering of blood sample	600	600
Sedimentation	1500	1500
Valve actuation	2700	150
Extraction of cancer cells	2700	450
Wash sample	3300	3300

the number of cells captured as well as the barrier properties of the absorbed cells. Fig. 3A shows cyclic voltammograms for a 1-mM solution of FeMeOH recorded with an on-disc gold electrode (dashed line), following modification with an anti-EpCAM capture layer (dotted line) and subsequent capture of 3.71×10^3 cells in PBS (solid line). Away from the formal potential, $E^{0\prime}$, (+0.06 V, determined from the mean of the anodic and cathodic peak potentials from the CV in Fig. 3A), the current is dominated by double-layer charging; the difference in current between the forward and backward wave depends on the interfacial capacitance. The interfacial capacitance at $U = -0.161$ V for the bare electrode, 70 ± 1 μF cm^{-2}, decreases to 48 ± 3 μF cm^{-2} for the anti-EpCAM coated electrode. This decrease in capacitance is consistent with adsorption of the antibody on the electrode surface that displaces solvent and ions. However, the magnitude of the change falls significantly short of that associated with the formation of a dense, close-packed film. This result suggests that ions and solvent can move through the antibody layer; hence, the layer is "leaky", i.e. displaying a low surface coverage with the antibody, thus promoting efficient binding of the target. Cell capture further decreases (by 42%) the capacitance to 40 ± 3 μF cm^{-2}, which is again consistent with impeded ion and solvent to the surface of the underlying electrode. Significantly, consistent with previous reports (Bard and Faulkner, 2001; Bourdillon et al., 1993; Kim et al., 2012; Venkatanarayanan et al., 2013), ESI – Figs. S4 and S5, the peak-to-peak separation for the oxidation of the ferrocene methanol does not change significantly following antibody immobilization suggesting that at the slow scan rate used, the rate of heterogeneous electron transfer to the ferrocene does not influence the voltammetric response. The peak current decreases marginally from 2.1 μA to 1.8 μA, suggesting that only a small fraction of the electrode area becomes inaccessible after antibody immobilization or the modified electrode behaves like a microelectrode array in which the active areas are close together and the diffusion fields overlap.

Cell capture can affect the voltammetric response in two distinct ways. First, captured cells may completely block electron transfer to the solution phase electroactive probe, thus reducing the effective electrode area and, correspondingly, the peak currents while maintaining the peak-to-peak separation, ΔU_P. Second, the captured cells may lower the rate of heterogeneous electron transfer causing ΔU_P to increase. Fig. 3A shows that the peak currents decrease marginally from 2.1 μA to 1.8 μA after the immobilization of the antibodies while ΔU_P remains unaffected. This result is consistent with the capacitance data and suggests the formation of a porous antibody capture layer; in an alternative picture, the modified electrode behaves like a microelectrode array in which the active areas are in close proximity so the diffusion fields overlap. Equally, the voltammetric current is insensitive to cell capture. However, confocal microscopy (Fig. 3D) confirms that relatively few cells are captured under these conditions. The most striking result of Fig. 3A is that, following deposition of the antibody layer, the formal potential of ferrocene increases by

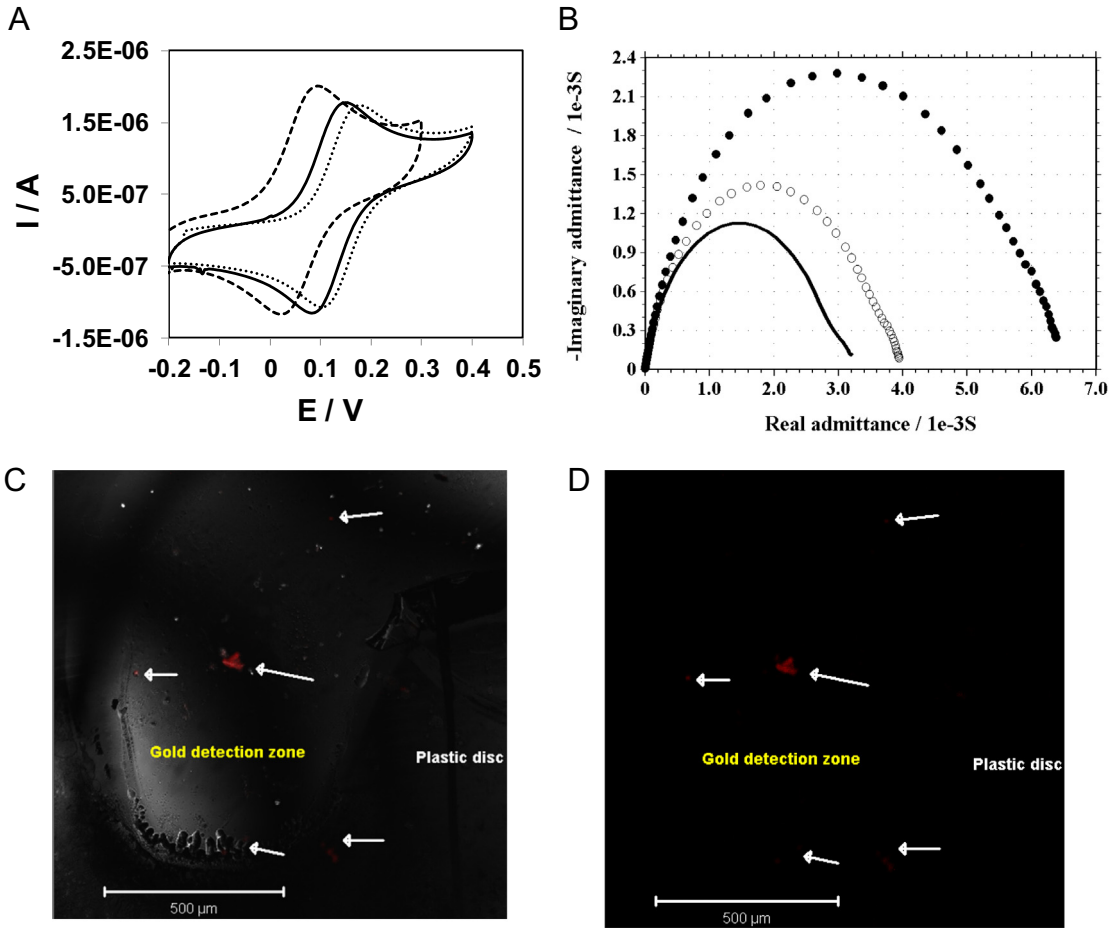

Fig. 3. (A) Cyclic voltammogram of bare on-disc gold electrode (dashed line), 100 µg/mL EpCAM antibody coated (dotted line) and 3.71×10^3 captured SKOV3 cells (solid line) in 1 mM FeOH in 0.001 M DPBS buffer, $\nu = 10$ mV s^{-1}, gold working and counter electrodes. (B) Nyquist admittance diagram of bare on-disc gold electrode (solid black line), 100 µg/mL EpCAM antibody coated (unfilled black circles) and captured SKOV3 cells (filled black circles) in 0.001 M DPBS buffer. The frequency range was 0.5 Hz to 100 kHz, the frequency increases from right to left, excitation signal of 50 mV peak amplitude was applied at open circuit potential. (C) Confocal fluorescence image emission and reflection channel. (D) Confocal fluorescence image emission channel alone of the corresponding electrode where the SKOV3 cells have been stained with 5 µM $DiOC_6$, excited at 488 nm and imaged with a 10× objective.

approximately 57 mV, indicating that it is harder to oxidize ferrocene in the presence of the antibody layer and even more after cell capture.

We have shown previously (Venkatanarayanan et al., 2013) that when the electrolyte concentration was high (0.1 M) the shape of the Nyquist response did not depend strongly on the antibody and cell concentration. However, in dilute electrolytes (0.001 M) the electrical double layer extends further out into solution and both the cell resistance and the capacitance depend on the antibody and cell concentration (surface coverage) – ESI – Figs. S4 and S5.

Initial experiments using the eLoaD platform were carried out in PBS buffer electrolyte. Fig. 3B shows the Nyquist admittance diagram of unmodified on-disc gold electrode (continuous black line), following modification with anti-EpCAM capture layer (unfilled black circles) and 3.71×10^3 captured cells in 0.001 M PBS buffer (filled black circles). It is evident that upon cell capture, as seen in Figs. 3C (emission and reflection channel) and 4D, (emission channel only) there is a significant increase in admittance value (Fig. 3B) from 3.0×10^{-3} S at unmodified on-disc gold electrode (solid black line) to 6.5×10^{-3} S at the same electrode with 3.71×10^3 cells in 0.001 PBS buffer (filled black circles). Cell capture is expected to augment the total electrochemical cell resistance. However, for this system the total impedance decreases following cell capture, indicating that the reduction in capacitance following cell capture is more significant than the increase in cell resistance.

Consequently, by tuning the double-layer thickness, and with the network of microfluidic channels on the eLoaD platform extracting the rare target cells, it is possible to detect low numbers of captured cancer cells. The anti-EpCAM modified eLoaD platform was exposed to 100 µL of diluted blood + Ficoll + DPBS that was spiked with concentrations of cancer cells between 1.9×10^5 and 1.5×10^8 cells/mL, pumped to the reaction chamber and then incubated for 3 h at room temperature.

3.3. CTC impedance assay, dynamic range and detection limit

The impedance response was measured as the concentration of cells in spiked blood was systematically varied. Fig. 4A shows the dependence of the impedance on the number of cancer cells captured. Fig. 4B displays the dependence of the relative change in impedance, Z_{REL} on the number of cells captured from blood sample. Z_{REL} is defined as

$$Z_{REL} = \mathrm{ABS}\left|\frac{Z_{Ab} - Z_C}{Z_{Ab} - Z_S}\right| \quad (1)$$

where ABS refers to the absolute value, Z_{Ab} and Z_C are the impedances observed for the anti-EpCAM antibody coated gold electrode and after exposure of these anti-EpCAM modified electrodes to SKOV3 cells of different concentrations, respectively. Z_S is the impedance observed for the highest surface coverage of

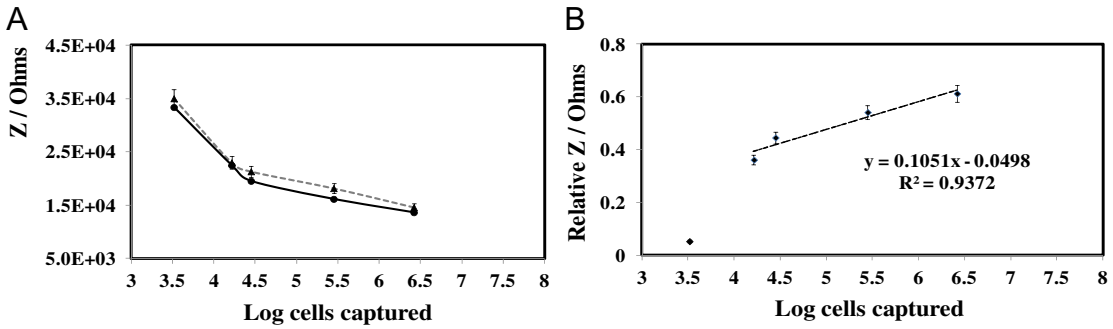

Fig. 4. (A) Plot showing the dependence of impedance on number of cancer cells specifically captured on centrifugal chip from 100 μL of diluted blood sample, with 0.001 M phosphate buffered saline electrolyte, gold working electrode and gold counter electrode at 117.2 Hz (solid line with filled circle) and 46.5 Hz (dotted line with filled triangle). (B) Graph showing the dependence of relative impedance on number of cancer cells specifically captured on centrifugal chip from100 μL of diluted blood sample, with 0.001 M phosphate-buffered saline electrolyte, gold working electrode and gold counter electrode at 117.2 Hz. The AC amplitude was 50 mV peak-to-peak and the DC potential was the open circuit potential and results were averaged over $n=5$ eLoaD platforms.

captured cells achieved i.e., as captured from a suspension containing 1.49×10^8 cells/mL.

Significantly, Fig. 4B demonstrates that Z_{REL} varies linearly with captured cell numbers at a frequency of 117.2 Hz and the eLoaD platform can detect circulating tumour cells over a wide linear dynamic range of 16,400–$(2.62 \pm 0.0003) \times 10^6$ cells. See S6—ESI for corresponding data. The smallest number of captured cells that could be reliably detected is 3270 cells corresponding to less than 214 cells/mm^2, i.e., this approach yields a measurable impedance change when approximately 2% of the electrode area is covered by SKOV3 cells.

On the basis of the calibration curve (Fig. 4A) the baseline impedance expected would be approximately 35 kΩ. The value of 2.5 kΩ observed following exposure of an unmodified electrode to the blood sample containing no SKOV3 cells is significantly lower; suggesting that exposure to blood significantly reduces the interfacial capacitance-most likely through non-specific adsorption of proteins. Control experiments in which the unmodified eLoaD platform was exposed to a suspension of SKOV3 cells containing 1.6×10^6 cells/mL demonstrate that captured cells are absent in confocal microscopy and the impedance cannot be distinguished from the bare gold surface. In contrast, exposing the antibody capture layer modified electrode to SKOV3 free blood raises the impedance, presumably due to an increase in resistance connected to the barrier properties of the non-specifically adsorbed proteins described above. However, the key result is that, as shown above for the clean buffer assays, the impedance decreases with a growing concentration of SKOV3 cells in the blood samples. As shown in Fig. 5, the total number of cells on an area of 15.3 mm^2 was estimated to be 2.803×10^4 cells. As 20 μL of input sample contained 3.2×10^4 cells, the capture efficiency of the LoaD platform was calculated to be 87%.

Significantly, these observations confirm that the impedance changes observed in Fig. 4 arise from *specific* binding of SKOV3 cells to anti-EpCAM antibodies on the eLoaD surface, and cannot be attributed to physisorption of other components that may be present in the cell suspension. For all cell coverages, an increase in frequency causes the overall magnitude of the impedance to decrease predominantly due to the lower capacitance of the interface following cell capture.

Fig. 5 shows confocal fluorescence images of the anti-EpCAM modified eLoaD electrodes after exposure to 1.6×10^6 cells/mL. These images clearly show the captured $DiOC_6$ labeled cells in the eLoaD channel containing the detection electrodes. It also reveals that the centrifugal platform specifically captures only cancer cells, i.e., the eLoaD platform successfully removes RBCs and only that

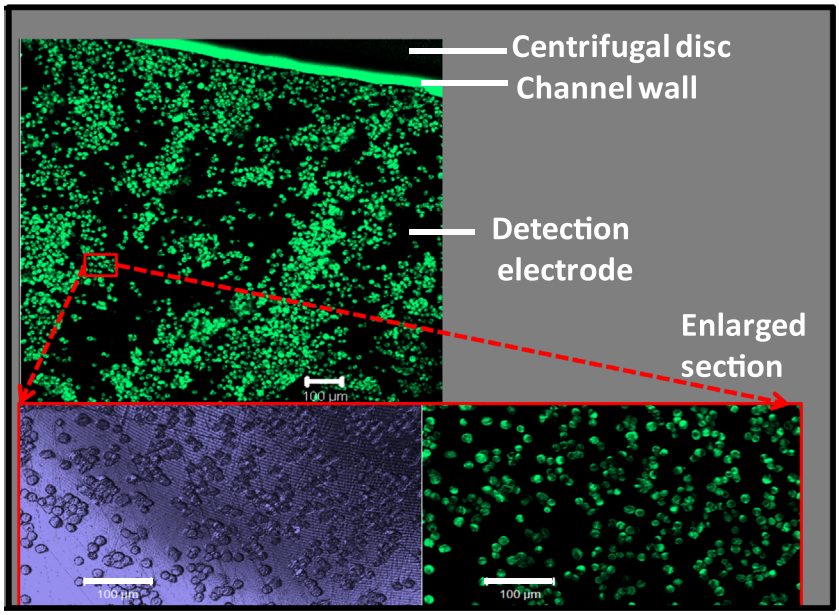

Fig. 5. Confocal fluorescence image of the captured SKOV3 cells on on-disc gold working electrode when disc was loaded with 1.6×10^6 cells/mL. The surface coverage on 15.3 mm^2 area electrode was estimated to be 2.8×10^4 cells. The cells were stained with 5 μM $DiOC_6$, excited at 488 nm and imaged with a 10 × objective, scale bar is 100 μm.

fraction of the plasma that contains cancer cells reaches the detection electrode where they are specifically captured. Other components of the plasma-like cell debris and platelets do not adhere to the anti-EpCAM modified gold electrodes and are washed away into the waste chamber.

4. Conclusions

We have for the first time demonstrated fully integrated liquid handling for the highly sensitive, label-free electrochemical detection of ovarian cancer cells (SKOV3) directly in whole blood using the eLoaD platform. The centrifugo-pneumatic DF valves in combination with the capillary-based siphon valving strategy automate sample preparation and assaying in the absence of any external pumping device. Significantly, applying an anti-EpCAM capture layer, low frequency AC signal (117.2 Hz) and open circuit DC potential, a detection limit of less than 214 ± 5 captured cells/mm^2 over a wide linear dynamic range of about three orders of magnitude and 87% capture efficiency was achieved. Given the large association constants that can be accomplished using engineered antibodies, this assay may be further improved to reach even lower detection limits.

Its proven versatility platform for other types of bioanalytical assays, e.g. on plasma-based biomarkers in blood, makes centrifugal eLoaD platform a promising candidate for establishing rapid, multi-parameter assays with microliter amounts of blood in common clinical settings, even at the point of care.

Acknowledgement

This work was supported by the Science Foundation Ireland (Grant nos. 10/CE/B1821, 12/TIDA/B2394 and 10/IN.1/B3021).

Appendix A. Supplementary material

Supplementary data associated with this article can be found in the online version at http://dx.doi.org/10.1016/j.bios.2014.12.049.

References

Abi-Samra, K., Kim, T.-H., Park, D.-K., Kim, N., Kim, J., Kim, H., Cho, Y.-K., Madou, M.J., 2013. Electrochemical velocimetry on centrifugal microfluidic platforms. Lab Chip 13 (16), 3253–3260.
Alix-Panabieres, C., Pantel, K., 2014. Technologies for detection of circulating tumor cells: facts and vision. Lab Chip 14 (1), 57–62.
Bard, A.J., Faulkner, L.R., 2001. Techniques Based on Concepts of Impedance. Electrochemical Methods: Fundamentals and Applications, 2nd edition John Wiley & Sons Inc, New York, p. 864.
Boettcher, M., Jaeger, M.S., Riegger, L., Ducrée, J., Zengerle, R., Duschl, C., 2006. Lab-on-chip-based cell separation by combining dielectrophoresis and centrifugation. Biophys. Rev. Lett. 1 (4), 443–451.
Bourdillon, C., Demaille, C., Gueris, J., Moiroux, J., Saveant, J.M., 1993. A fully active monolayer enzyme electrode derivatized by antigen–antibody attachment. J. Am. Chem. Soc. 115 (26), 12264–12269.
Burger, R., Ducrée, J., 2012. Handling and analysis of cells and bioparticles on centrifugal microfluidic platforms. Expert Rev. Mol. Diagn. 12 (4), 407–421.
Burger, R., Kirby, D., Glynn, M., Nwankire, C., O'Sullivan, M., Siegrist, J., Kinahan, D., Aguirre, G., Kijanka, G., Gorkin 3rd, R.A., Ducree, J., 2012. Centrifugal microfluidics for cell analysis. Curr. Opin. Chem. Biol. 16 (3–4), 1–6.
Chen, Q.L., Cheung, K.L., Kong, S.K., Zhou, J.Q., Kwan, Y.W., Wong, C.K., Ho, H.P., 2012. An integrated lab-on-a-disc for automated cell-based allergen screening bioassays. Talanta 97 (0), 48–54.
Coumans, F.A.W., van Dalum, G., Beck, M., Terstappen, L.W.M.M., 2013. Filtration parameters influencing circulating tumor cell enrichment from whole blood. PLoS One 8 (4), e61774.
Dotan, E., Cohen, S.J., Alpaugh, K.R., Meropol, N.J., 2009. Circulating tumor cells: evolving evidence and future challenges. Oncologist 14 (11), 1070–1082.
Ducrée, J., Haeberle, S., Lutz, S., Pausch, S., Stetten, Fv, Zengerle, R., 2007. The centrifugal microfluidic Bio-Disk platform. J. Micromech. Microeng. 17 (7), S103–S115.
Duford, D.A., Xi, Y., Salin, E.D., 2013. Enzyme inhibition-based determination of pesticide residues in vegetable and soil in centrifugal microfluidic devices. Anal. Chem. 85 (16), 7834–7841.
Focke, M., Stumpf, F., Roth, G., Zengerle, R., von Stetten, F., 2010. Centrifugal microfluidic system for primary amplification and secondary real-time PCR. Lab Chip 10 (23), 3210–3212.
Gorkin III, R., Nwankire, C.E., Gaughran, J., Zhang, X., Donohoe, G.G., Rook, M., O'Kennedy, R., Ducrée, J., 2012. Centrifugo-pneumatic valving utilizing dissolvable films. Lab Chip 12 (16), 2894–2902.
Gorkin, R., Park, J., Siegrist, J., Amasia, M., Lee, B.S., Park, J.M., Kim, J., Kim, H., Madou, M., Cho, Y.K., 2010. Centrifugal microfluidics for biomedical applications. Lab Chip 10 (14), 1758–1773.
Greiner, C., Hunter, M., Rius, F., Huang, P., Georgakoudi, I., 2011. Confocal back-scattering-based detection of leukemic cells in flowing blood samples. Cytometry Part A 79A (10), 874–883.
Grumann, M., Brenner, T., Beer, C., Zengerle, R., Ducrée, J., 2005. Visualization of flow patterning in high-speed centrifugal microfluidics. Rev. Sci. Instrum. 76 (2), 025101–025106.
Hou, H.W., Warkiani, M.E., Khoo, B.L., Li, Z.R., Soo, R.A., Tan, D.S., Lim, W.T., Han, J., Bhagat, A.A., Lim, C.T., 2013. Isolation and retrieval of circulating tumor cells using centrifugal forces. Sci. Rep. 3, 1259.
Hun, X., Chen, H., Wang, W., 2010. Design of ultrasensitive chemiluminescence detection of lysozyme in cancer cells based on nicking endonuclease signal amplification technology. Biosens. Bioelectron. 26 (1), 248–254.
Ignatiadis, M., Kallergi, G., Ntoulia, M., Perraki, M., Apostolaki, S., Kafousi, M., Chlouverakis, G., Stathopoulos, E., Lianidou, E., Georgoulias, V., Mavroudis, D., 2008. Prognostic value of the molecular detection of circulating tumor cells using a multimarker reverse transcription-PCR assay for cytokeratin 19, mammaglobin A, and HER2 in early breast cancer. Clin. Cancer Res. 14 (9), 2593–2600.
Jemal, A., Bray, F., Center, M.M., Ferlay, J., Ward, E., Forman, D., 2011. Global cancer statistics. CA: Cancer J. Clin. 61 (2), 69–90.
Jin, C., McFaul, S.M., Duffy, S.P., Deng, X., Tavassoli, P., Black, P.C., Ma, H., 2014. Technologies for label-free separation of circulating tumor cells: from historical foundations to recent developments. Lab Chip 14 (1), 32–44.
Kim, T.-H., Park, J., Kim, C.-J., Cho, Y.-K., 2014. Fully Integrated lab-on-a-disc for nucleic acid analysis of food-borne pathogens. Anal. Chem. 86 (8), 3841–3848.
Kim, Y.-P., Park, S., Lee, D., Kim, H.-S., 2012. Electrochemical glucose biosensor by electrostatic binding of PQQ–glucose dehydrogenase onto self-assembled monolayers on gold. J. Appl. Electrochem. 42 (6), 383–390.
Kinahan, D.J., Kearney, S.M., Glynn, M.T., Ducrée, J., 2014. Spira mirabilis enhanced whole blood processing in a lab-on-a-disk. Sens. Actuators A: Phys. 215, 71–76.
Kumeria, T., Kurkuri, M.D., Diener, K.R., Parkinson, L., Losic, D., 2012. Label-free reflectometric interference microchip biosensor based on nanoporous alumina for detection of circulating tumour cells. Biosens. Bioelectron. 35 (1), 167–173.
Law, W.-C., Yong, K.-T., Baev, A., Prasad, P.N., 2011. Sensitivity improved surface plasmon resonance biosensor for cancer biomarker detection based on plasmonic enhancement. ACS Nano 5 (6), 4858–4864.
Lee, A., Park, J., Lim, M., Sunkara, V., Kim, S.Y., Kim, G.H., Kim, M.-H., Cho, Y.-K., 2014a. All-in-one centrifugal microfluidic device for size-selective circulating tumor cell isolation with high purity. Anal. Chem. 86 (22), 11349–11356.
Lee, S., Chon, H., Lee, J., Ko, J., Chung, B.H., Lim, D.W., Choo, J., 2014b. Rapid and sensitive phenotypic marker detection on breast cancer cells using surface-enhanced Raman scattering (SERS) imaging. Biosens. Bioelectron. 51 (0), 238–243.
Lianidou, E., Markou, A., Strati, A., 2012. Molecular characterization of circulating tumor cells in breast cancer: challenges and promises for individualized cancer treatment. Cancer Metastasis Rev. 31 (3–4), 663–671.
Loutherback, K., apos, Silva, J., Liu, L., Wu, A., Austin, R.H., Sturm, J.C., 2012. Deterministic separation of cancer cells from blood at 10 mL/min. AIP Adv. 2 (4), 042107.
Madou, M., Zoval, J., Guangyao, J., Kido, H., Kim, J., Kim, N., 2006. Lab on a CD. Annu. Rev. Biomed. Eng. 8, 601–628.
Nagrath, S., Sequist, L.V., Maheswaran, S., Bell, D.W., Irimia, D., Ulkus, L., Smith, M.R., Kwak, E.L., Digumarthy, S., Muzikansky, A., Ryan, P., Balis, U.J., Tompkins, R.G., Haber, D.A., Toner, M., 2007. Isolation of rare circulating tumour cells in cancer patients by microchip technology. Nature 450 (7173), 1235–1239.
Nwankire, C., Chan, D.-S., Gaughran, J., Burger, R., Gorkin, R., Ducrée, J., 2013a. Fluidic automation of nitrate and nitrite bioassays in whole blood by dissolvable-film based centrifugo-pneumatic actuation. Sensors 13 (9), 11336–11349.
Nwankire, C.E., Donohoe, G.G., Zhang, X., Siegrist, J., Somers, M., Kurzbuch, D., Monaghan, R., Kitsara, M., Burger, R., Hearty, S., Murrell, J., Martin, C., Rook, M., Barrett, L., Daniels, S., McDonagh, C., O'Kennedy, R., Ducrée, J., 2013b. At-line bioprocess monitoring by immunoassay with rotationally controlled serial siphoning and integrated supercritical angle fluorescence optics. Anal. Chim. Acta 781 (0), 54–62.
Nwankire, C.E., Czugala, M., Burger, R., Fraser, K.J., O'Connell, T.M., Glennon, T., Onwuliri, B.E., Nduaguibe, I.E., Diamond, D., Ducrée, J., 2014. A portable centrifugal analyser for liver function screening. Biosens. Bioelectron. 56 (0), 352–358.
Pantel, K., Brakenhoff, R.H., Brandt, B., 2008. Detection, clinical relevance and specific biological properties of disseminating tumour cells. Nat. Rev. Cancer 8 (5), 329–340.

Park, J.M., Lee, J.Y., Lee, J.G., Jeong, H., Oh, J.M., Kim, Y.J., Park, D., Kim, M.S., Lee, H.J., Oh, J.H., Lee, S.S., Lee, W.Y., Huh, N., 2012. Highly efficient assay of circulating tumor cells by selective sedimentation with a density gradient medium and microfiltration from whole blood. Anal. Chem. 84 (17), 7400–7407.

Scher, H.I., Jia, X., de Bono, J.S., Fleisher, M., Pienta, K.J., Raghavan, D., Heller, G., 2009. Circulating tumour cells as prognostic markers in progressive, castration-resistant prostate cancer: a reanalysis of IMMC38 trial data. Lancet Oncol. 10 (3), 233–239.

Sheng, W., Chen, T., Kamath, R., Xiong, X., Tan, W., Fan, Z.H., 2012. Aptamer-enabled efficient isolation of cancer cells from whole blood using a microfluidic device. Anal. Chem. 84 (9), 4199–4206.

Siegrist, J., Gorkin, R., Clime, L., Roy, E., Peytavi, R., Kido, H., Bergeron, M., Veres, T., Madou, M., 2010. Serial siphon valving for centrifugal microfluidic platforms. Microfluid. Nanofluid. 9 (1), 55–63.

Tan, S., Yobas, L., Lee, G., Ong, C., Lim, C., 2009. Microdevice for the isolation and enumeration of cancer cells from blood. Biomed. Microdevices 11 (4), 883–892.

Venkatanarayanan, A., Keyes, T.E., Forster, R.J., 2013. Label-free impedance detection of cancer cells. Anal. Chem. 85 (4), 2216–2222.

Vila-Planas, J., Fernandez-Rosas, E., Ibarlucea, B., Demming, S., Nogues, C., Plaza, J.A., Dominguez, C., Buttgenbach, S., Llobera, A., 2011. Cell analysis using a multiple internal reflection photonic lab-on-a-chip. Nat. Protoc. 6 (10), 1642–1655.

Wicha, M.S., Hayes, D.F., 2011. Circulating tumor cells: not all detected cells are bad and not all bad cells are detected. J. Clin. Oncol. 29 (12), 1508–1511.

Zheng, S., Lin, H.K., Lu, B., Williams, A., Datar, R., Cote, R.J., Tai, Y.-C., 2011. 3D microfilter device for viable circulating tumor cell (CTC) enrichment from blood. Biomed. Microdevices 13 (1), 203–213.